Research Article

Improvement in Corrosion Inhibition Efficiency of Molybdate-Based Inhibitors via Addition of Nitroethane and Zinc in Stimulated Cooling Water

Saeed Mohammadi, Fatemeh Baghaei Ravari, and Athareh Dadgarinezhad

Department of Materials Science and Engineering, Faculty of Engineering, Shahid Bahonar University, Kerman 7618868366, Iran

Correspondence should be addressed to Saeed Mohammadi, s_mohammadi@alumni.ut.ac.ir

An investigation was conducted to improve the corrosion inhibition efficiency of molybdate-based inhibitors for mild steel which is the main construction material of cooling water systems, using nitroethane as an organic compound beside zinc. In this study a new molybdate-based inhibitor was introduced with the composition of 60 ppm molybdate, 20 ppm nitrite, 20 ppm nitroethane, and 10 ppm zinc. Inhibition efficiency of molybdate alone and with nitrite, nitroethane, and zinc on the uniform corrosion of mild steel in stimulated cooling water (SCW) was assessed by electrochemical techniques such as potentiodynamic polarization and electrochemical impedance (AC impedance) measurements. Weight loss measurements were made with coupon testing specimens in the room temperature for 48 h. Studies of electron microscopy, including scanning electron microscopy (SEM) photograph and X-ray energy dispersive spectrometry (EDS) microanalysis, were used. The results obtained from the polarization and AC impedance curves were in agreement with those from the corrosion weight loss results. The results indicate that the new inhibitor is as effective as molybdate alone, though at one-ninth of the concentration range of molybdate, which is economically favorable.

1. Introduction

The protection of cooling water systems as well as heat supply water has become one of the great important issues in the world economy. The application of corrosion inhibitors especially in closed systems holds a prominent place amongst other methods of corrosion control [1]. The actual trends in the environmental protection essentially have changed the traditional approach to corrosion inhibition. Since the toxicity of chromate-based inhibitor is a limiting factor in its use as a corrosion inhibitor, the changes in formulation of corrosion inhibitors are prompted primarily by an increasing demand to reduce environmental impact [2]. Molybdate-based inhibitor has long been known as an inorganic and anodic type of corrosion inhibitor, which is effective for protecting mild steel in the pH range 5.8–8.5 [3, 4]. Lizlovs has observed that in the aqueous system containing aggressive ions, molybdate has corrosion inhibition only in the presence of oxygen [5]. In fact, the presence of aggressive ions such as chloride (Cl^-) and sulfate (SO_4^{-2}) anions reduces the efficiency of MoO_4^{2-}, so higher concentrations are necessary for corrosion inhibition [6, 7], which is not economically favorable. In order to achieve better efficiency and reduce the quantity of molybdate, other oxidizing agents such as nitrite (NO_2^-) and organic compounds have been employed. Recently, the best method to improve inhibitive capability is using inhibitors in combination with others [8–11]. As it has been observed previously, organic inhibitors usually designated as a film forming protect the metal by forming a hydrophobic film on the metal surface. Therefore, natural organic molecules containing one pair of electrons or associated with multiple specially triple bonds or organic rings can bond to metal surface by electron transfer to the metal to form a coordinate type of link,
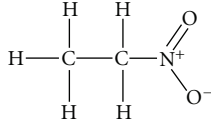
FIGURE 1: Molecular structure of sodium nitroethane.

TABLE 1: Chemical composition of test specimen.

Element	C	Si	Mn	Fe
Test specimen	0.05	0.49	0.54	98.92

which ultimately produces a barrier to the dissolution of the metal in the electrolyte [12]. As nitroethane contains a carbon chain together with oxidizing agent (NO_2^-), it is predicted that it can improve inhibition efficiency as an organic compound. In addition, Jefferies and Bucher recently studied the addition of zinc as cathodic inhibitor to improve the corrosion inhibition behavior of molybdate-based inhibitors [13]. As a result, it is worth investigating the corrosion inhibition of mild steel in stimulated cooling water (SCW) by using new developed inhibitor containing molybdate, nitrite, nitroethane, and zinc.

2. Experimental Procedures

Coupon testing specimens with the dimensions of 5, 2, and 0.3 cm were used for weight loss measurements. The composition of mild steel specimens is shown in Table 1.

Mild steel of the same alloy composition with an exposed area of $1 cm^2$ was embedded in epoxy resin and used for electrochemical measurements. Tafel polarization measurements were carried out at open circuit potential (E_{ocp}), potentiostat/galvanostat (Princeton Applied Research EG & G Model 263 A), using counter electrode (Pt) and a saturated calomel electrode (SCE) as reference electrode. All the quoted potentials are referred to this reference electrode. The potentiodynamic current-potential curves were carried out at a scan rate 1 mV/sec. For impedance measurement, the same equipment was used for the Tafel polarization measurement and combined with frequency response analyzer (Princeton Model 1020). The impedance measurement was carried out using AC signals of amplitude 10 mV peak to peak at the open circuit potential in the frequency range 100 KHz to 10 mHz. Before each test, the specimens were prepared with silicon carbide paper 220–1200 grit, degreased in acetone, and washed in distilled water. Test solutions with different inhibitors (Table 2) were prepared by dissolving analytical grade sodium molybdate (Na_2MoO_4), sodium nitrite ($NaNO_2$), zinc sulfate ($ZnSO_4$), and sodium nitroethane ($C_2H_5NNaO_2$).

Figure 1 shows the molecular structure of sodium nitroethane. Distilled water with 500 ppm sodium chloride, 520 ppm sodium sulfate, 170 ppm sodium bicarbonate, and 25 ppm sodium carbonate was used as SCW [14].

TABLE 2: Chemical composition of inhibitors.

| Inhibitor	Concentrations (ppm)
1000M	1000 Molybdate sodium
40N	40 Nitrite sodium
20Ne	20 Nitroethane sodium
60M40N	60 Molybdate sodium + 40 nitrite sodium
40N20Ne	40 Nitrite sodium + 20 nitroethane sodium
60M20Ne	60 Molybdate sodium + 20 nitroethane sodium
60M40N10Zn	60 Molybdate sodium + 40 nitrite sodium + 10 zinc sulfate
60M20Ne10Zn	60 Molybdate sodium + 20 nitroethane sodium + 10 zinc sulfate
60M20N20Ne10Zn	60 Molybdate sodium + 20 nitrite sodium + 20 nitroethane sodium + 10 zinc sulfate
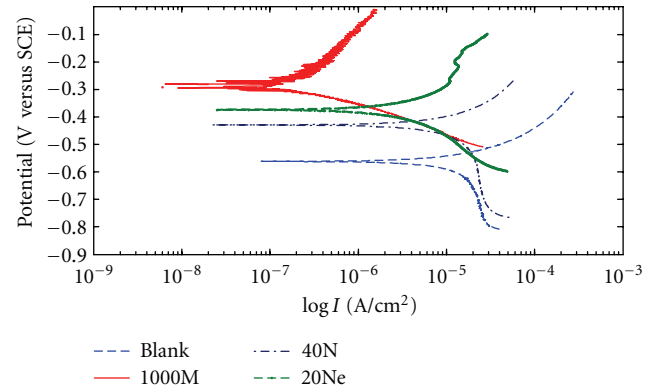
FIGURE 2: Polarization curves for mild steel in SCW without inhibitor and with inhibitor 1000 ppm molybdate, 40 ppm nitrite, and 20 ppm nitroethane.

All tests were performed at neutral pH and room temperature. Before measurements of polarization curves, a stabilization period of 20 min was observed which proved sufficient as indicated by open circuit potential (E_{ocp}). Table 2 shows the composition of different inhibitors used in this work.

The surface morphology of the mild steel samples after immersion in SCW without inhibitor and with inhibitor 1000 M and the new optimized inhibitor was photographed using SEM and was analyzed by EDS (Cam Scan 2300 MV).

3. Results and Discussion

3.1. Polarization Curves. The anodic and cathodic polarization curves for mild steel in SCW without inhibitor and with different inhibitors are shown in Figures 2–5. Figure 2 shows polarization curves for mild steel without inhibitor and with inhibitor 1000 ppm molybdate, 40 ppm nitrite, and 20 ppm nitroethane.

TABLE 3: Electrochemical polarization parameters for mild steel in SCW without inhibitor and with different inhibitors.

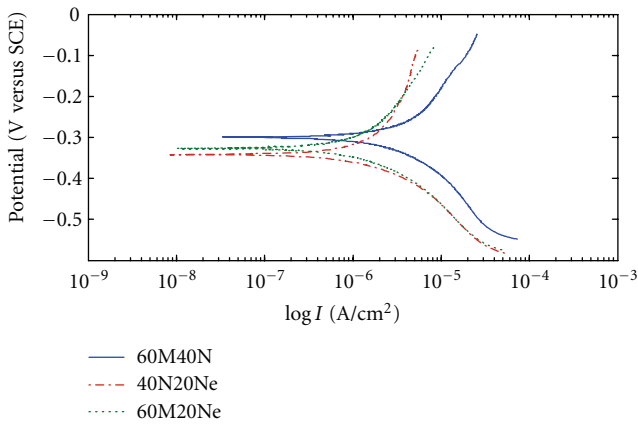| Inhibitor	E_{corr} (mV)	βc (mV/dcade)	βa (mV/dcade)	I_{corr} ($\mu A/cm^2$)	η (%)
Blank	−550	135	325	14.5	—
1000M	−285	78	187	0.186	98.6
40N	−471	154	188	5.6	61.4
20Ne	−380	98	103	1.82	87.4
60M40N	−308	141	137	1.63	88.7
40N20Ne	−340	68	74	0.83	94.3
60M20Ne	−330	108	153	0.59	96
60M40N10Zn	−318	103	86	0.7	95.2
60M20Ne10Zn	−336	79	144	0.23	98.2
60M20N20Ne10Zn	−298	90	196	0.173	98.8

FIGURE 3: Polarization curves for mild steel exposed to mixture of 60 ppm molybdate and 40 ppm nitrite, 40 ppm nitrite and 20 ppm nitroethane, and 60 ppm molybdate and 20 ppm nitroethane.

The addition of 1000 ppm molybdate, 40 ppm nitrite, and 20 ppm nitroethane shifted the corrosion potentials of the mild steel to more positive values and also decreased the corrosion current densities (I_{corr}), indicating that molybdate, nitrite, and nitroethane are anodic inhibitors.

Table 3 gives values of corrosion potentials (E_{corr}), corrosion current densities (I_{corr}), Tafel slopes (βc and βa), and inhibition efficiency (η%) obtained from polarization measurements of mild steel for different inhibitors in SCW. The corrosion current densities were obtained from the polarization curves by linear extrapolation of Tafel curves at point of 50 mV more positive and 50 mV more negative than E_{ocp}, respectively.

The inhibition efficiency is defined as

$$\eta(\%) = \frac{I_{corr} - I_{corr(i)}}{I_{corr}} \times 100, \qquad (1)$$

where I_{corr} and $I_{corr(i)}$ are the corrosion current density values without inhibitor and with different inhibitors, respectively.

For the curve 1000 M, corrosion current density is 0.185 ($\mu A/cm^2$), indicating a negligible corrosion rate. But it is not suitable because the concentration is high. According to the obtained results, molybdate was considered as a weak oxidizer, so other oxidizing agents such as nitrite and nitroethane were added to molybdate in order to achieve better efficiency and reduce the quantity of molybdate.

Figure 3 exhibits the polarization curves for mild steel exposed to mixture of 60 ppm molybdate and 40 ppm nitrite, 40 ppm nitrite and 20 ppm nitroethane, and 60 ppm molybdate and 20 ppm nitroethane.

According to the curves 60M40N, a concentration of 60 ppm MoO_4^{2-} and 40 ppm NO_2^- appeared to be more efficient than molybdate and nitrite alone at mentioned concentrations [11]. Also by considering curve 40N20Ne, one should point out that in solution containing both nitrite and nitroethane ions, anodic curves were shifted to more positive values compared with nitrite and nitroethane alone, indicating synergistic behavior and improvement in the inhibition efficiency. According to Figure 2, nitroethane with half of the concentration range of nitrite exhibits better inhibition corrosion efficiency. So the combination of 60 ppm molybdate and 20 ppm nitroethane was used in order to achieve better efficiency and reduce the corrosion current densities of Tafel curve 60M40N.

Considering the fact that cathodic inhibitors improve the corrosion inhibition efficiency and reduce the corrosion current densities, combination of zinc with mixture of 60 ppm molybdate and 40 ppm nitrite and mixture of 60 ppm molybdate and 20 ppm nitroethane was used to improve the corrosion inhibition efficiency of Tafel curves 60M40N and 60M20Ne, as shown in Figure 4.

According to the Tafel curves 60M40N10Zn and 60M20Ne10Zn, addition of zinc (with delay to cathodic reactions) to oxidizing agents such as molybdate, nitrite, and nitroethane improves the corrosion inhibition efficiency and reduce the corrosion current densities of mild steel specimens in SCW. Moreover, addition of zinc to Tafel curves 60M40N and 40N20Ne shifts the cathodic and anodic branches of the Tafel plots to less corrosion current values (I_{corr}) at relatively the same corrosion potentials, indicating that zinc acts as cathodic inhibitor besides other anodic inhibitors.

Polarization curves for mild steel were exposed to SCW water by adding molybdate, nitrite, nitroethane, and zinc
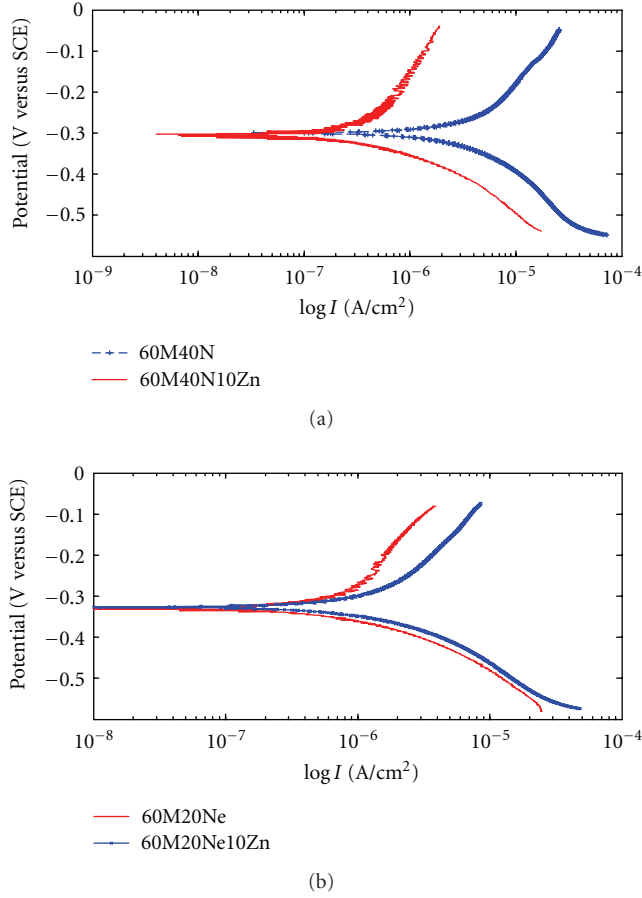
(a)

(b)

FIGURE 4: Polarization curves for mild steel in SCW by adding zinc to (a) 60 ppm molybdate and 40 ppm nitrite, curve 60M40N10Zn and (b) 40 ppm nitrite and 20 ppm nitroethane, curve 40N20Ne10Zn.

(60 ppm, 20 ppm, 20 ppm, and 10 ppm, resp.), and 1000 ppm molybdate alone is shown in Figure 5. For comparison polarization curves in SCW and without inhibitor are included.

The suitable combination of $MoO_4^{2-} + NO_2^-$ beside nitroethane and zinc ions provides the necessary oxidizing environment to support MoO_4^{2-} film formation and synergically lower the corrosion rate. This combination also overcomes the high concentration of MoO_4^{2-}, with relatively the same E_{corr}, which is economically favorable. Also for optimized inhibitor current density was on the order of 0.173 ($\mu A/cm^2$), which was lowered by about 6.9% compared with 1000 ppm molybdate alone. It can be attributed to the absorption of other ions on the metal in conjunction with MoO_4^{2-} to produce an insoluble compound, providing passivity more readily than MoO_4^{2-} alone [11].

Regarding these results, it can be concluded that the value of corrosion of current density of mild steel in SCW with the addition of molybdate decreases, and with addition of nitrite, nitroethane, and zinc ions to molybdate it decreases more and its inhibition efficiency increases.
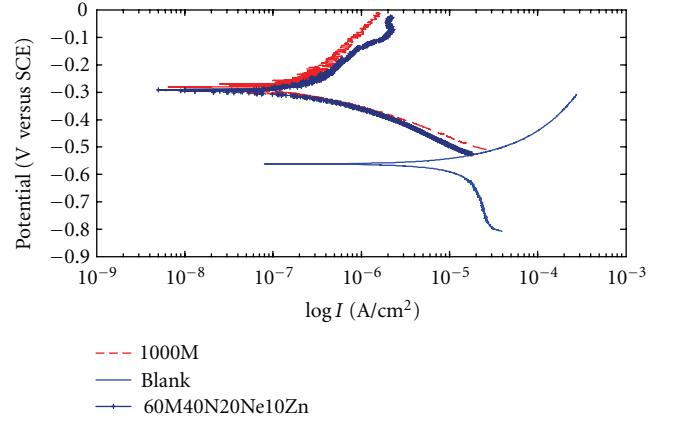

FIGURE 5: Polarization curves for mild steel in SCW without inhibitor and with inhibitor 1000 M and new optimized inhibitor.

TABLE 4: AC impedance parameters for mild steel in SCW without inhibitor and with different inhibitors.

| Inhibitor	R_{ct} ($\Omega \cdot cm^2$)	η (%)
Blank	1068	—
1000M	16345	93.5
40N	1650	56.8
20Ne	4470	76.1
60M40N	4513	76.6
40N20Ne	4518	76.8
60M20Ne	7083	84.9
60M40N10Zn	4720	77.4
60M20Ne10Zn	7360	85.5
60M20N20Ne10Zn	17205	93.8

3.2. AC Impedance Curves. Figures 6 and 7 show the Bode and Bode phase plots of steel electrode without inhibitor and with different inhibitors. The main effect of different inhibitors is an increase in the impedance modulus, $|z|$, below 10 mHz (an increase in polarization resistance (R_p)) and also a higher phase angle.

In Bode phase plots, only one peak is in the phase angle (α) versus frequency (f) plot, indicating that there is only one time constant (a single relaxation time constant).

Figure 8 shows Nyquist plots for the steel electrode in SCW solutions without inhibitor and with different inhibitors. The impedance loops measurements were depressed semicircles with their center below the axis. This phenomenon is known as the dispersing effect [15]. In Nyquist plots, the corrosion resistance of each of the samples was determined by R_p. R_p is given by [16]

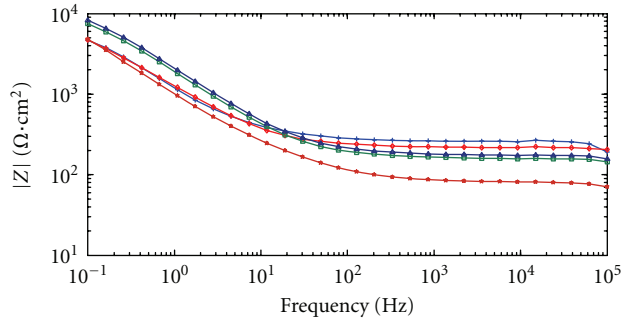$$R_p = \lim_{\omega \to 0} R_e \left\{ Z_f \right\}_{E=E_{corr}}, \qquad (2)$$

where $R_e\{Z_f\}$ represents the real part of the complex faradic impedance, Z_f and ω correspond to the angular velocity of the AC signal ($\omega = 2\pi f$, where f is frequency, (Hz)). R_p values were obtained by fitting the experimental Nyquist data to a simple semicircle and extrapolating to $Z_{im} = 0$.
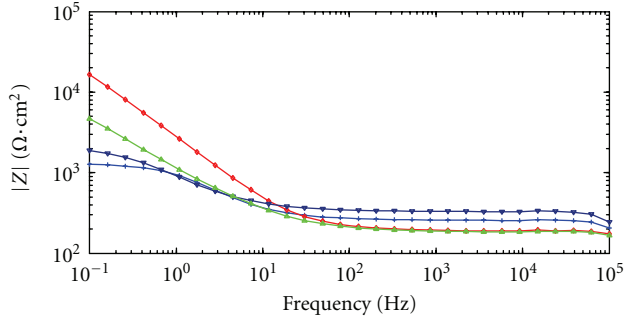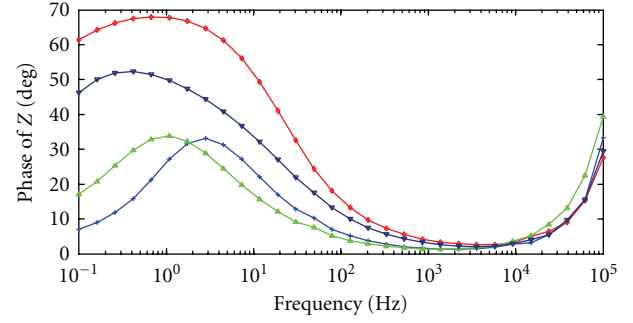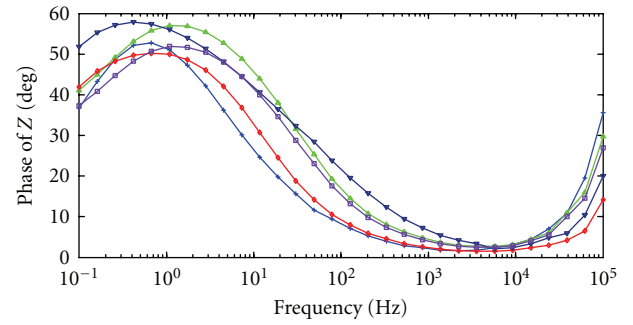
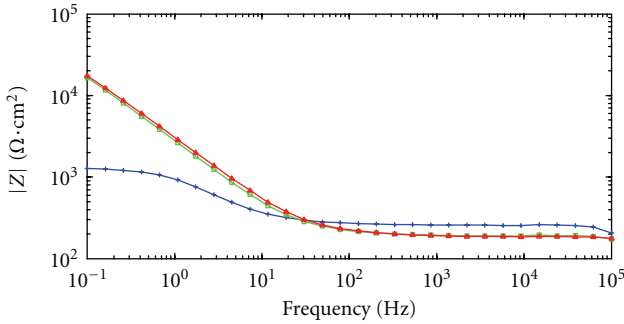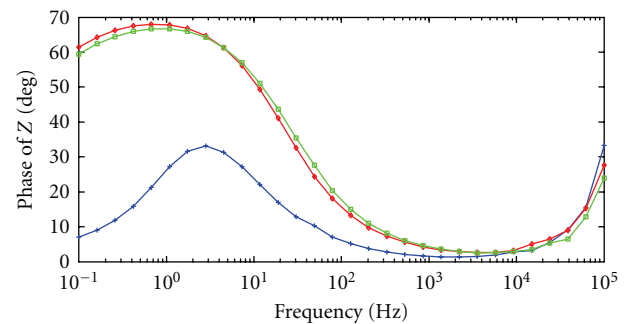FIGURE 6: Bode plots for mild steel in SCW solution (a) without inhibitor and with different inhibitor.

FIGURE 7: Bode phase plots for mild steel in SCW solution without inhibitor and with inhibitor.

By considering AC impedance curves, it was found that polarization resistance increases in the following order.

BLANK < 40N < 20Ne < 40N20Ne ≈ 60M40N < 60M40N10Zn < 60M20Ne < 60M20Ne10Zn < 1000 M ≤ 60M20N20Ne10Zn.

Table 4 gives the values of inhibition efficiency ($\eta\%$) and polarization resistance (R_{ct}) obtained from the AC impedance measurements. The inhibition efficiency is defined as

$$\eta \ (\%) = \frac{R_{ct(i)} - R_{ct}}{R_{ct(i)}} \times 100, \qquad (3)$$

where R_{ct} and $R_{ct(i)}$ are the polarization resistance without inhibitor and with different inhibitors, respectively.
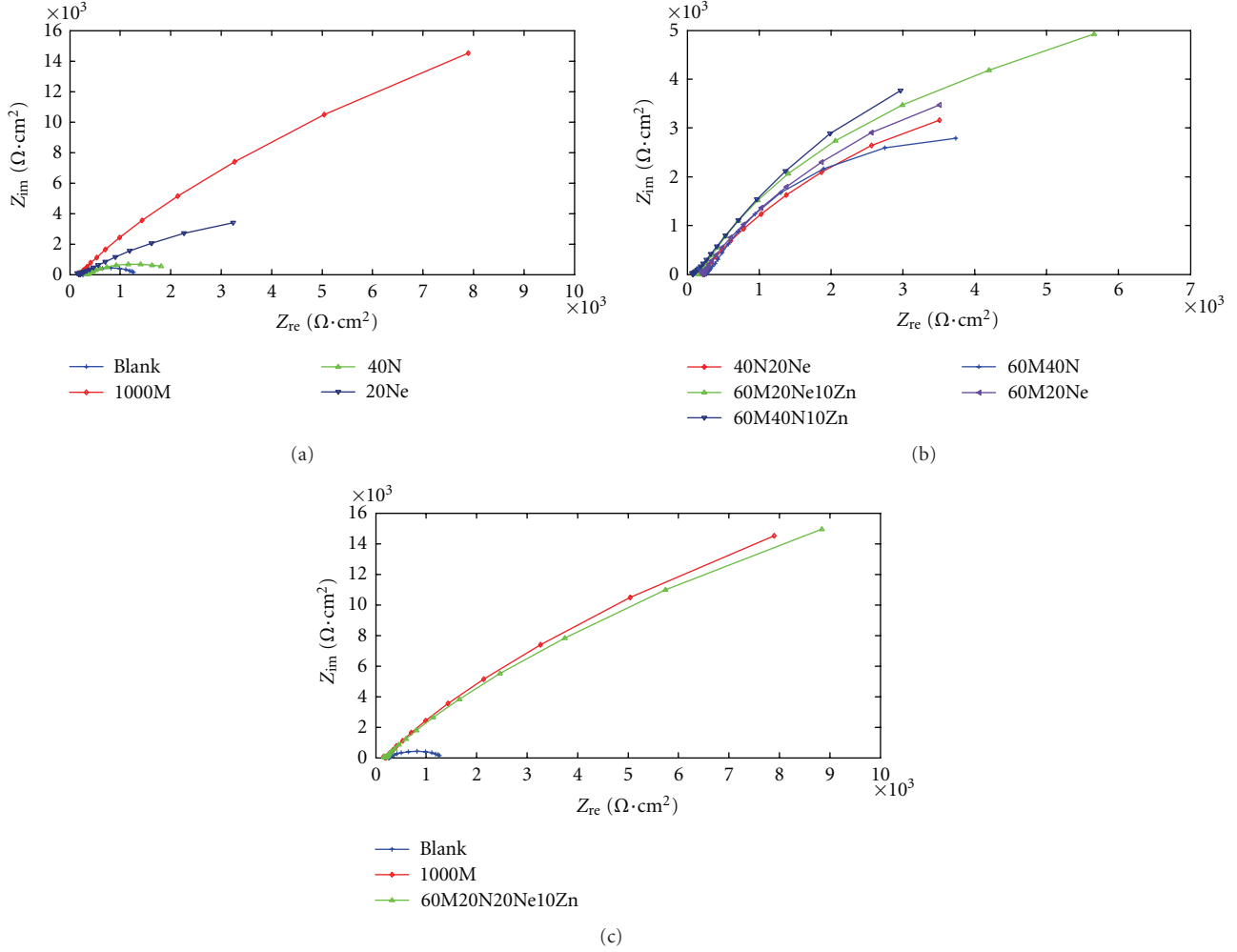
(a)

(b)

(c)

FIGURE 8: Nyquist plots for mild steel in SCW solution without inhibitor and with inhibitor.

TABLE 5: Weight loss measurements for mild steel in SCW without inhibitor and with different inhibitors.

Inhibitor	η (%)
Blank	—
1000M	86.5
40N	49.7
20Ne	69.2
60M40N	70.1
40N20Ne	69.8
60M20Ne	78
60M40N10Zn	70.6
60M20Ne10Zn	78.8
60M20N20Ne10Zn	86.8

The results of the AC impedance test exhibit a good correlation with data obtained from the polarization curves.

3.3. Weight Loss Measurements.

The weight loss of samples after 48 h exposure to solution SCW without inhibitor and with different inhibitors was measured by coupon testing methods [17]. Regarding experimental weight loss data, inhibition efficiency (η%) was calculated classically as follows:

$$\eta(\%) = \frac{W_0 - W_i}{W_0} \times 100, \tag{4}$$

where W_0 and W_i are the weight loss observed in the absence and in the presence of inhibitor, respectively. Values of inhibition efficiency for mild steel in SCW without inhibitor and with different inhibitors are summarized in Table 5.

For comparison, the inhibition efficiency of polarization, AC impedance, and weight loss results were summarized in Figure 9. According to Figure 9, the results obtained from the polarization and AC impedance curves are in agreement with those from the corrosion weight loss tests.

3.4. Results of Surface Analysis Techniques

3.4.1. SEM Analysis.

The presence of corrosion inhibitor could be more clearly investigated by means of surface analysis techniques. SEM micrographs of samples after 48 h
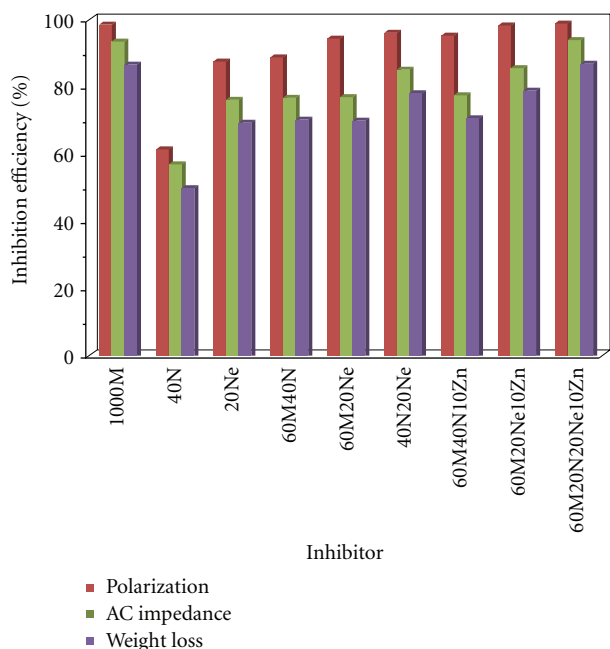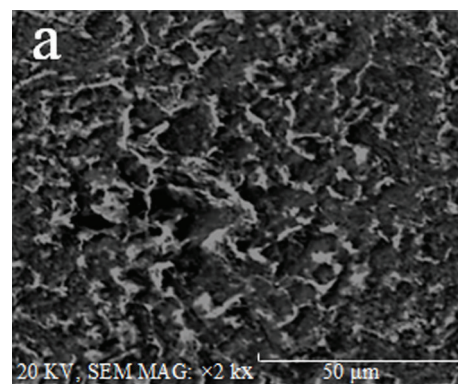
FIGURE 9: The inhibition efficiency of polarization, AC impedance, and weight loss results for mild steel in SCW with different inhibitors.

(a)

(b)

(c)

FIGURE 10: SEM micrograph for mild steel surface (a) in SCW without inhibitor, (b) in SCW with the inhibitor 1000 M, and (c) in SCW with new optimized inhibitor.

exposure to (a) solution SCW without inhibitor, (b) solution SCW with inhibitor 1000 M, and (c) solution SCW with new optimized inhibitor are shown in Figure 10. Figures 10(b) and 10(c) exhibit a layer with uniform, adherent, and continuous structure, while Figure 10(a) shows crystal growth of iron oxide on the surface and its noncontinuous structure. In fact, the decrease in corrosion current densities and increase in polarization resistance when exposed to the previous inhibitors were due to the coverage of metal surface with more protective films [18] as shown in Figure 10. Also the surface roughness of mild steel exposed to solution SCW is much higher than mild steel exposed to solution SCW with the inhibitor 1000 M and optimized inhibitor.
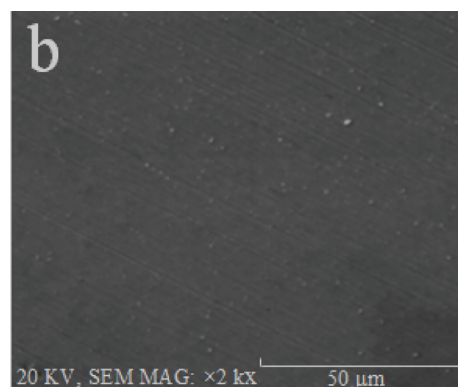
3.4.2. EDS Analysis. EDS analysis of samples after 48 h exposure to solution SCW without inhibitor and with inhibitor 1000 ppm molybdate and new optimized inhibitor is shown in Figure 11. The presence of C, Si, Mn, and Fe element can be observed in all figures. But the presence of Mo is only in Figures 11(b) and 11(c), indicating that molybdate oxide is formed on the surface of mild steel sample as stabilizer through its incorporation into the oxide film [18].

In addition, as shown in Figure 11(c), the carbon peak is much higher than (1000 ppm) molybdate alone, indicating that nitroethane ions are adsorbed on the surface besides molybdate ions to improve its inhibition efficiency synergically.
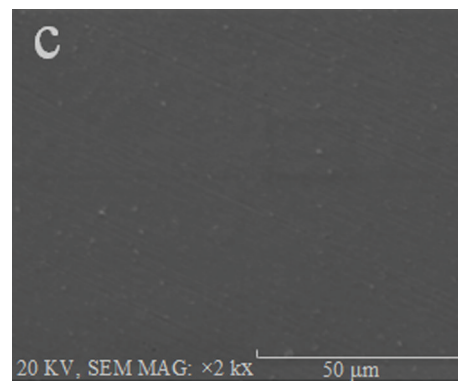
Finally, a glance at the electrochemical (polarization, AC impedance and weight loss method) and surface analysis (SEM photograph and EDS microanalysis) results indicates that new optimized inhibitor has relatively better efficiency

than 1000 ppm molybdate alone at one ninth of the concentration range of molybdate, which is economically favorable.

4. Conclusions

(1) MoO_4^{2-} was proved to be a weak oxidizer, so another oxidizing agents such as NO_2^- and nitroethane beside cathodic inhibitor zinc were shown to be required to provide adequate protection for mild steel in stimulated cooling water.
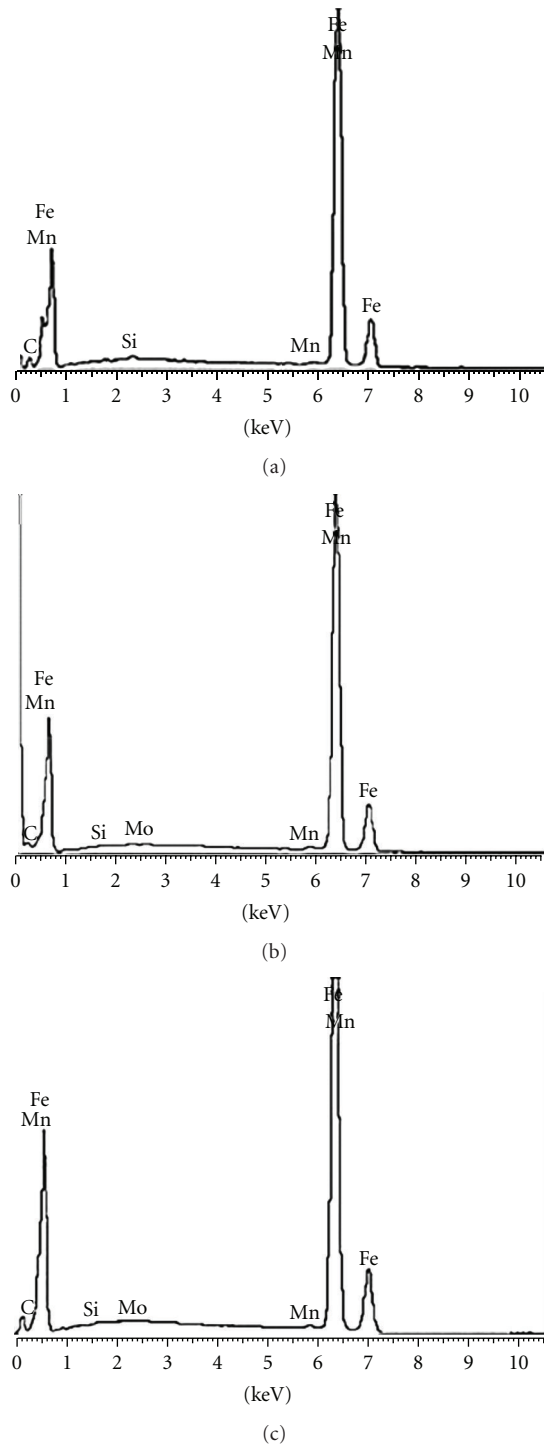
(a)

(b)

(c)

FIGURE 11: EDS analysis of mild steel (a) in SCW without inhibitor, (b) in SCW with inhibitor 1000 M, and (c) in SCW with new optimized inhibitor.

(2) Results obtained from polarization curves showed that new optimized inhibitor with more than 98 percent inhibition efficiency noticeably lowers the corrosion rate of mild steel in stimulated cooling water.

(3) AC impedance curves showed that the combination of molybdate, nitrite, and nitroethane, beside cathodic inhibitor zinc in optimized range can be a suitable replacement for high concentration of 1000 ppm molybdate.

(4) The results of weight loss measurements obtained from coupon testing specimens exhibit a good correlation with data obtained from the polarization and AC impedance curves.

(5) The presence of molybdate as stabilizer of oxide film is observed through the EDS analyzer.

(6) SEM images indicate that new optimized inhibitor could form a relatively steady, compact, and uniform film on the surface of mild steel.

References

[1] C. M. Mustafa and J. P. G. Farr, "A potentiodynamic study of the corrosion inhibition of mild steel in realistic situation by molybdate and organic compounds containing –COOH and/or –OH groups," *Indian Journal of Technology*, vol. 30, p. 424, 1992.

[2] O. Lahodny-Sarc, F. Kapor, and R. Halle, "Corrosion inhibition of carbon steel in chloride solutions by blends of calcium gluconate and sodium benzoate," *Materials and Corrosion*, vol. 51, no. 3, pp. 147–151, 2000.

[3] Y. J. Qian and S. Turgoose, "Inhibition by zinc-molybdate mixtures of corrosion of mild steel," *British Corrosion Journal*, vol. 22, no. 4, pp. 268–271, 1987.

[4] M. J. Pryor and M. Cohen, "The inhibition of the corrosion of iron by some anodic inhibitors," *Journal of the Electrochemical Society*, vol. 100, pp. 203–215, 1953.

[5] E. A. Lizlovs, "Molybdates as corrosion inhibitors in the presence of chlorides," *Corrosion*, vol. 32, no. 7, pp. 263–266, 1976.

[6] P. A. Burda, "Molybdates as chromate replacement for closed cooling. Water systems in nuclear industry," *Corrosion*, vol. 92, p. 118, 1992.

[7] M. A. Stranick, "Corrosion inhibition of metals by molybdate. Part I. mild steel," *Corrosion*, vol. 40, no. 6, pp. 296–302, 1984.

[8] A. J. Bentley, L. G. Earwaker, J. P. G. Farr, and A. M. Seeney, "A technique for the in situ elemental analysis of electrode surfaces," *Surface Technology*, vol. 23, no. 1, pp. 99–103, 1984.

[9] J. P. G. Farr and M. Saremi, "Molybdate in aqueous corrosion inhibition I: effects of molybdate on the potentiodynamic behaviour of steel and some other metals," *Surface Technology*, vol. 19, no. 2, pp. 137–144, 1983.

[10] C. M. Mustafa and S. M. S. I. Dulal, "Molybdate and nitrite as corrosion inhibitors for copper-coupled steel in simulated cooling water," *Corrosion*, vol. 52, no. 1, pp. 16–22, 1996.

[11] D. B. Alexander and A. A. Moccari, "Evaluation of corrosion inhibitors for component cooling water systems," *Corrosion*, vol. 49, no. 11, pp. 921–928, 1993.

[12] V. S. Sastri, *Corrosion Inhibitors. Principles and Applications*, John Wiley & Sons, Toronto, Canada, 1998.

[13] J. Jefferies and B. Bucher, "New look at molybdate," *Materials Performance*, vol. 31, no. 5, pp. 50–53, 1992.

[14] S. Karim, C. M. Mustafa, M. D. Assaduzzman, and M. Islam, "Effect of nitrate ion on corrosion inhibition of mild steel

in simulated cooling water," *Chemical Engineering Research Bulletin*, vol. 14, pp. 87–91, 2010.

[15] F. Mansfeld, M. W. Keding, and S. Tsai, "Recording and analysis of AC impedance data for corrosion studies-experimental approach and results," *Corrosion*, vol. 38, p. 301, 1982.

[16] W. J. Lorenz and F. Mansfeld, "Determination of corrosion rates by electrochemical DC and AC methods," *Corrosion Science*, vol. 21, no. 9-10, pp. 647–672, 1981.

[17] ASTM, "Standard practice for laboratory immersion corrosion testing of metal," ASTM International G 31-72, West Conshohocken, Pa, USA, 1990.

[18] S. M. A. Shibli and V. A. Kumary, "Inhibitive effect of calcium gluconate and sodium molybdate on carbon steel," *Anti-Corrosion Methods and Materials*, vol. 51, no. 4, pp. 277–281, 2004.